

## Evaluation of Absolute Photoabsorption Cross Sections of an Endohedral Metallofullerene, Pr@C<sub>82</sub>

H. Katayanagi<sup>1,2</sup>, B. P. Kafle<sup>2</sup>, T. Mori<sup>1</sup>, J. Kou<sup>1</sup>, Y. Takabayashi<sup>3</sup>, E. Kuwahara<sup>3</sup>,  
Y. Kubozono<sup>3</sup>, K. Mitsuke<sup>1,2</sup>

<sup>1</sup>*Department of Vacuum UV Photo-Science, Institute for Molecular Science, Okazaki 444-8585 Japan*

<sup>2</sup>*Graduate University for Advanced Studies, Okazaki 444-8585 Japan*

<sup>3</sup>*Department of Chemistry, Okayama University, Okayama 700-8530 Japan*

We measured yield curves of photoions produced by the photoionization of an endohedral metallofullerene, Pr@C<sub>82</sub>, and reported the result last year [1]. Figure 1 shows the yield curves of doubly (a) and singly (b) charged photoions. In Fig. 1, a peak accompanied by an oscillatory structure is discernible at around 130 eV. In [1], we concluded that the peak originated from the giant resonance of encapsulated Pr atoms and that the oscillatory structure implies an interference effect by the fullerene cage. To make clear these phenomena more quantitatively, we evaluated absolute photoabsorption cross sections of Pr@C<sub>82</sub> from the photoion yield curves.

The experimental technique to obtain the yield curves was described in detail elsewhere [2]. Briefly, a Pr@C<sub>82</sub> beam was generated by sublimation in vacuum and ionized by the synchrotron radiation in the photon energy range of 100 – 150 eV; photoions were observed by time-of-flight mass spectrometer.

The photoabsorption cross sections to produce singly and doubly charged ions can be expressed by the formula [3]:

$$\sigma(\text{Pr@C}_{82}^{z+}) = R(\text{Pr@C}_{82}^{z+}) \Phi n L \eta f \tau \quad (1)$$

$R(\text{Pr@C}_{82}^{z+})$  is the count rate of the ion signals of Pr@C<sub>82</sub><sup>z+</sup>,  $\Phi$  is the photon flux of synchrotron radiation,  $n$  is the number density of Pr@C<sub>82</sub> in the ionization region,  $L$  is the length of the ionization volume along the light path,  $\eta$  is the overall detection efficiency of the apparatus,  $f$  is the repetition rate of the pulsed electric field applied to the ionization region and  $\tau$  is the average residence time of the ions in the ionization volume. We can obtain the above values directly from the experiment except the detection efficiency,  $\eta$ . We used C<sub>60</sub> as a standard sample to estimate  $\eta$ . We evaluated total photoabsorption cross sections by summing up the cross sections to produce singly and doubly charged ions since signal intensities of triply and higher charged ions were found to be very low. Here we assumed that the quantum yield for photoionization is equal to unity in the photon energy range used.

The values of the cross sections at on- and off-resonance energies are listed in Table 1. Lengthy discussion on the validity of an evaluation method used and the accuracy of the cross sections is omitted here and can be found elsewhere [4]. The difference between the cross sections at 110 and 130 eV is 16.5

Mb. This value corresponds to an enhancement by the giant resonance. The value agrees well with that of Ce@C<sub>82</sub> (14.3Mb). Since a typical value of cross sections of the lanthanide atom is 40 – 50 Mb, the giant resonance was found to be suppressed by the fullerene cage in Pr@C<sub>82</sub> as well as in Ce@C<sub>82</sub> [2].

From the present study on Pr@C<sub>82</sub>, we found that the existence (and the suppression) of the giant resonance is not just a characteristic of Ce@C<sub>82</sub> sample and can be a tendency of metallofullerenes. Furthermore, we are designing a more intense fullerene beam source to obtain the oscillatory structure with higher reproducibility. Such spectra will allow us to apply an analysis method similar to that used in XAFS spectroscopy to make clear local structures and charge distributions around interior metal atoms. The analysis will complement results obtained by the X-ray powder diffraction.

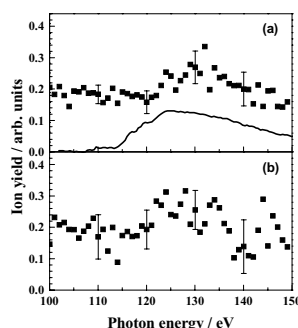


Fig. 1 Ion yield curves of (a) Pr@C<sub>82</sub><sup>2+</sup> and (b) Pr@C<sub>82</sub><sup>+</sup>. Error bars correspond to 1 $\sigma$  of five experimental runs. Solid curve in (a) is the absorption spectrum of Pr atoms.

Table 1 Cross sections of Pr@C<sub>82</sub> at the photon energy of 110 and 130 eV. All cross sections are in Mb. Numbers in parentheses show estimated errors.

Photon energy	cross section		
	Pr@C <sub>82</sub> <sup>+</sup>	Pr@C <sub>82</sub> <sup>2+</sup>	Total
110 eV (off-resonance)	5.8 (2.6)	14.1 (6.1)	19.8 (7.3)
130 eV (on-resonance)	10.6 (3.2)	25.6 (6.4)	36.3 (9.2)

[1] H. Katayanagi *et al.*, UVSOR Activity Report **2004** (2005) 51.

[2] K. Mitsuke *et al.*, J. Chem. Phys. **122** (2005) 064304.

[3] T. Mori *et al.*, J. Electron Spectrosc. Relat. Phenom. **144 – 147** (2005) 243.

[4] H. Katayanagi *et al.*, in preparation.

## Orbital-Dependent Stabilization in the Valence Ionization of CS<sub>2</sub> Cluster

T. Hatsui<sup>1</sup>, J. Plenge<sup>2</sup>, E. Rühl<sup>2</sup>, N. Kosugi<sup>1</sup>

<sup>1</sup>*Dept. of Vacuum UV photoscience, Institute for Molecular Science, Okazaki 444-8585 Japan*

<sup>2</sup>*Physical and Theoretical Chemistry, Freie Universität Berlin, Takustr. 3, 14195 Berlin*

Van der Waals clusters have been interested since they give opportunities to investigate the connection between isolated and condensed phases. Cluster formation is known to give the decrease in adiabatic binding energy, which is commonly interpreted in terms of final state polarization stabilization, where the created hole upon ionization polarizes the surrounding atom/molecules. The polarization stabilization is dependent on the distance to the surrounding atoms/molecules and their polarizability. In the case of valence ionization of molecular clusters, valence holes are generally delocalized within the molecule, where the shape of the hole is characteristic of the valence molecular orbital (MO). In this study, we have investigated the stabilization effect in CS<sub>2</sub> cluster in order to observe MO dependent stabilization of the valence ionized states.

CS<sub>2</sub> cluster was produced by a continuous supersonic jet expansion with seeding He gas. The jet is intersected with a beam of linearly polarized soft X-rays from the in-vacuum undulator beam line BL3U with an energy resolving power  $E/\Delta E$  better than 1000 at 65 eV photon energy. Electrons are analyzed at 55° to the electric vector of the incident x-rays by a Scienta SES-200 hemispherical analyzer and an MBS A-1 control system (A1\_200\_#86) with path energy of 20 V.

The photoelectron spectra of CS<sub>2</sub> molecule and the mixture of CS<sub>2</sub> molecule and cluster are presented in Fig. 1. The mixture spectrum clearly shows broad bands at the binding energy lower than the bare molecule bands. The cluster spectrum is obtained by subtracting the molecular spectrum. The cluster spectrum arises from clusters with different sizes. In the case of larger mean size with increased stagnation pressure, the peaks of the cluster bands are shifted toward the lower binding energy. The band profile indicates the abundance of the cluster in terms of their size. The peak position of each band can be regarded as the vertical binding energy at certain cluster size. In order to observe the dependence of the energy shift on the ionized states, higher resolution photoelectron spectra are measured by using He I source. The obtained spectrum is similarly subtracted to obtain the cluster spectrum, and plotted in relative energy scale, where zero energy is chosen to be the vertical energy of each ionized states for molecule (Fig. 2). X band has the peak maximum around relative binding energy of -0.6 eV. The relative binding energies are increased in order of X, A, B, and C. It is probable that vibrational progression of each ionized states does not change upon the cluster formation because the progressions are mainly determined by the

potentials associated with the intra-molecular vibrational modes. The results therefore indicate that ionized state with lower binding energy has smaller stabilization effect. The polarization for low-lying ionized states with a delocalized valence hole is expected to give smaller stabilization. This trend is consistent with the present observation. In summary, the energies of the valence ionized states in CS<sub>2</sub> cluster are determined by the polarization stabilization, which is dependent on the MO character of the holes.

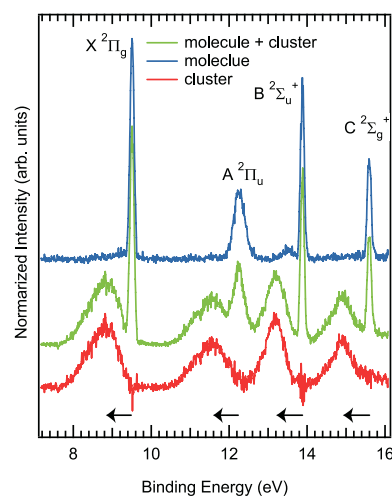


Fig. 1 Photoelectron spectra of CS<sub>2</sub> molecule, the mixture of molecule and cluster, and the cluster. Arrows indicate the decrease of the binding energy upon cluster formations.

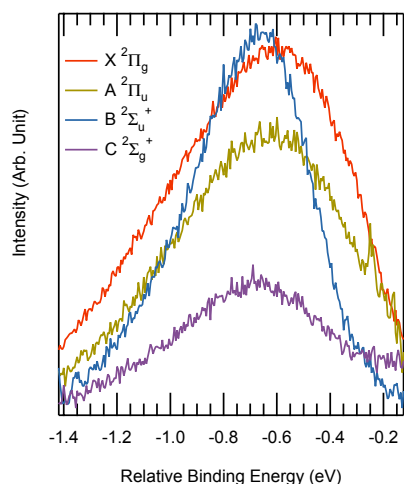


Fig. 2 Valence bands for cluster relative to the vertical binding energy of the corresponding states in molecule.

## Efficient Production of Metastable Fragments around the 1s Ionization Threshold in N<sub>2</sub>

Y. Hikosaka<sup>1</sup>, P. Lablanquie<sup>2</sup>, E. Shigemasa<sup>1</sup>

<sup>1</sup>*UVSOR Facility, Institute for Molecular Science, Okazaki 444-8585 Japan*

<sup>2</sup>*Laboratoire de Chimie Physique-Matière et Rayonnement, 75231 Paris Cedex 05 France*

Photoionization dynamics at small excess energy from the inner-shell threshold of an atom or a molecule, closely relates to post-collision interaction (PCI), *i.e.* the interaction between photoelectron, Auger electron and the atomic field which changes during the process. The PCI effect is exhibited on both the energy distributions of photoelectrons and Auger electrons. When the photon energy is tuned close to the inner-shell threshold, PCI can lead the photoelectron to be recaptured into a Rydberg orbital. The photoelectron recapture results in singly-charged ions in high-*n* Rydberg states. This phenomenon has been relatively well studied for atoms but rarely for molecules. In this work, we have measured the yields of neutral species, in the vicinity of the 1s ionization threshold of N<sub>2</sub> [1]. The present work demonstrates the neutral particle observation can be a new probe for investigating the dynamics on the photoelectron recapture in molecules.

The neutral particle yield spectrum in  $h\nu=405.8-412$  eV of N<sub>2</sub> is displayed in Fig. 1, in comparison with an ion yield spectrum. Below the 1s threshold, the structures corresponding to Rydberg excitations are seen on both spectra. An intriguing characteristic of the neutral particle yield spectrum is the large peak around the 1s threshold, which is absent from the ion yield spectrum. The large peak lies at  $h\nu=410.0$  eV, just above the 1s ionization threshold, which results from the detection of metastable fragments N\* [1].

For the N\* formation below the 1s threshold, we propose the following mechanism whose reaction sequence is illustrated in Fig. 2. A high-*n* Rydberg state converging to N<sub>2</sub><sup>+</sup>(1s)<sup>-1</sup> is populated by photoexcitation (Reaction 1). The subsequent resonant Auger decay from this high-*n* Rydberg state results in an N<sub>2</sub><sup>+</sup> state, where spectator Auger decay is more favored due to the weak interference between the core hole and the high-*n* Rydberg electron (Reaction 2). After the spectator Auger decay, the Auger final state is a singly-charged high-*n* Rydberg state converging to an N<sub>2</sub><sup>2+</sup> state. Since most N<sub>2</sub><sup>2+</sup> states are dissociative, it is very likely that the high-*n* Rydberg N<sub>2</sub><sup>+</sup> state dissociates into N<sup>+</sup> + N\* (Reaction 3), due to the parallelism between the potential energy curves of the high-*n* Rydberg N<sub>2</sub><sup>+</sup> state and the N<sub>2</sub><sup>2+</sup> state. The resulting N\* should be in a high-*n* Rydberg state, and can be detected by our neutral particle detector.

The large peak on the neutral particle yield spectrum clearly shows a tail to the higher photon

energy side. The tail is interpreted in terms of the PCI effect. The reaction sequence of the N\* formation due to PCI is also illustrated in Fig. 2. At the 1s threshold, and above, a slow photoelectron is emitted (Reaction 1'). The formed 1s core-hole usually decays non-radiatively and emits a fast Auger electron. The fast Auger electron overtakes the slow photoelectron, which results in a decrease of the kinetic energy of the photoelectron. The shift of the photoelectron energy can exceed the initial energy given at the photoionization, and the photoelectron can be recaptured into a high-*n* Rydberg orbital (Reaction 2'). The resultant N<sub>2</sub><sup>+</sup> in a high-*n* Rydberg state may produce an N\* fragment (Reaction 3). This process appears as the tail seen on the neutral particle yield spectrum

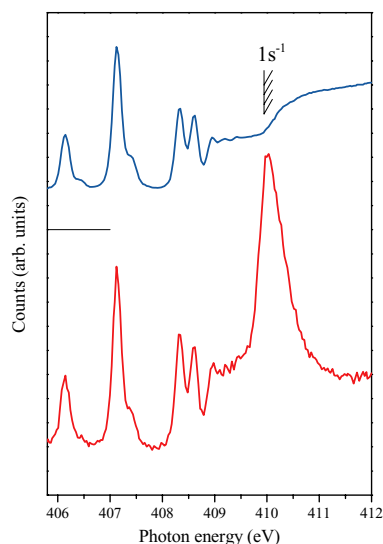


Fig. 1 Ion yield (blue) and neutral particle yield (red) in N<sub>2</sub>.

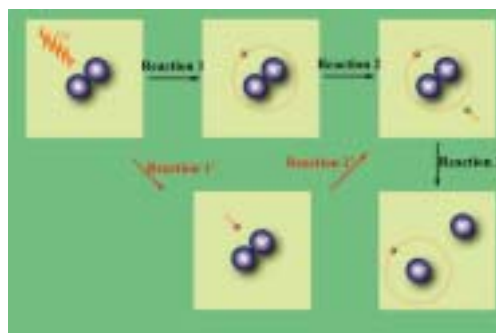


Fig. 2 Reaction sequence for the N\* formation.

[1] Y. Hikosaka *et al.*, J. Phys. B **38** (2005) 3597.

# Coster-Kronig Decay of HCl Studied by the Threshold Photoelectron-Auger Electron Coincidence Spectroscopy

T. Kaneyasu<sup>1</sup>, T. Aoto<sup>2</sup>, Y. Hikosaka<sup>1</sup>, E. Shigemasa<sup>1</sup>, K. Ito<sup>2</sup>

<sup>1</sup>*UVSOR Facility, Institute for Molecular Science, Okazaki 444-8585 Japan*

<sup>2</sup>*Photon Factory, Institute of Materials Structure Science, Tsukuba 305-0801 Japan*

Inner-shell ionization and its subsequent Auger decay produce doubly ionized states. Auger electron spectroscopy has been one of the useful experimental methods to investigate the doubly ionized states of atoms and molecules, because the kinetic energy of the Auger electron corresponds to the transition energy from the initial core-hole state to the final doubly ionized state. The interpretation of the Auger spectrum often becomes, however, difficult in the conventional Auger spectroscopy, mainly due to the following two reasons. The first one is the so-called lifetime broadening of the Auger peaks, resulting from the life time of the initial core-hole state due to the uncertainty principle ( $\Delta E=100$  meV  $\leftrightarrow$   $\Delta T=6.5$  fs). Secondly, it is difficult to observe the individual Auger lines separately, when the Auger lines associated with various core-hole states and their satellites are superimposed.

In order to overcome such difficulties, coincidence Auger spectroscopy has been emerged where an Auger electron and a photoelectron are detected simultaneously. The coincidence detection enables to select the initial core-hole state associated with the Auger lines. Furthermore, the natural linewidth of the core-hole state does not affect the spectral resolution of the coincidence Auger spectrum, which can be better than the natural linewidth of the initial core-hole state. The spectral resolution is determined only by the experimental condition when the kinetic energies of both the Auger electron and the photoelectron are measured.

So far we have applied the coincidence Auger spectroscopy to rare gases and an H<sub>2</sub>S molecule (see *e.g.* [1] and references therein) by detecting a threshold photoelectron as a counter part of Auger electrons. The experimental procedure of the threshold photoelectron-Auger electron coincidence spectroscopy has already been described in the paper [2]. In this work, we have firstly measured weak Cl 2s Coster-Kronig Auger lines of HCl. Figure 1 shows the yield of threshold photoelectrons against the photon energy measured in the vicinity of the Cl 2s threshold. The spectral structures in Fig. 1 are corresponding to the excitation and ionization processes of the Cl 2s electron. The first peak at 271.5 eV is attributed to the excitation to the 3p $\sigma^*$  orbital. The second one around 276 eV is owing to the unresolved Rydberg states. The threshold electron yield reaches its maximum at 279.5 eV, which should relate to the Cl 2s photoionization. The ionization energy of the Cl 2s is however determined to be 278.0 eV. Such difference can be explained by the

post-collision interaction effect, namely, the slower photoelectron is overtaken by the Auger electron.

The Cl 2s coincidence/normal Auger spectra are presented in Fig. 2. It is obvious that the Auger lines are clearly resolved in the coincidence spectrum, in contrast to the normal Auger spectrum. The spectral resolution is expected to be 0.5 eV in the coincidence spectrum, which is well below the natural linewidth of the Cl 2s core-hole state (1.8 eV). However, any sharp structures can hardly be seen in the coincidence spectrum. This may indicate that many doubly ionized states with (Cl 2p)<sup>-1</sup>(V)<sup>-1</sup> configurations lie in the energy region of Fig. 2, and are overlapped. The two major structures at 233 eV and 237 eV are probably due to the formation of HCl<sup>2+</sup> [(Cl 2p)<sup>-1</sup>(V)<sup>-1</sup>] states with 2 $\pi$  and 5 $\sigma$  valence holes, respectively.

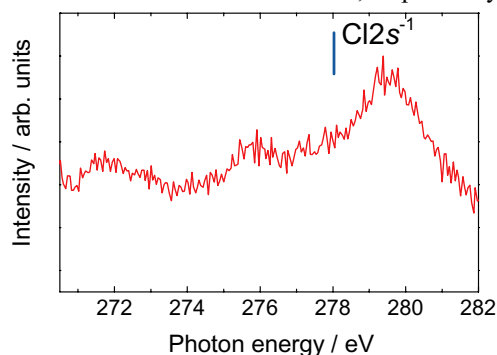


Fig. 1 Threshold photoelectron spectrum of HCl measured in vicinity of the Cl 2s threshold.

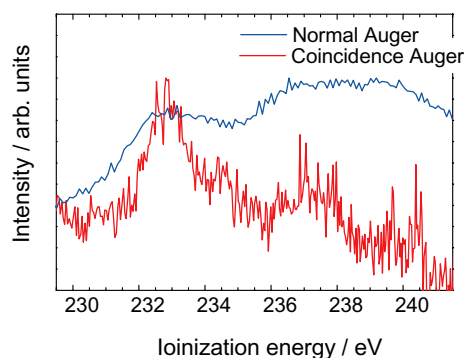


Fig. 2 Cl 2s Coster-Kronig Auger spectra of HCl measured at  $h\nu=357.5$  eV for normal Auger, and at  $h\nu=279.5$  eV for coincidence Auger spectrum.

[1] Y. Hikosaka *et al.*, J. Electron Spectrosc. Relat. Phenom. **133-140** (2004) 287.

[2] Y. Hikosaka *et al.*, Meas. Sci. Tech. **11** (2000) 1697.

## Double Toroidal Electron Analyzer for Auger Electron-Ion Coincidence Experiments

T. Kaneyasu, Y. Hikosaka, E. Shigemasa

*UVSOR Facility, Institute for Molecular Science, Okazaki 444-8585 Japan*

A double toroidal type electron analyzer (DTA) has been constructed for studies on anisotropic electron emission following molecular inner-shell photoionization. The analyzer, which is based on the high luminosity electron spectrometer originally developed by the French group [1], allows simultaneous measurements of angular distributions and energy distributions of electrons utilizing a two-dimensional position sensitive detector (PSD). The acceptance solid angle is 5% of  $4\pi$  sr and electrons within the energy range 10% of the pass energy can be observed. A three-dimensional view of our DTA is shown in Fig. 1, which consists of a four element conical electrostatic lens, two toroidal shaped deflectors and PSD. The conical symmetry of the lens system defines the detection angle of  $54.7^\circ$  with respect to the analyzer symmetrical axis. The ejected electrons are focused by the four element lens system and energy dispersed by the toroidal deflectors. The electrons are finally detected by PSD. The pass energy of DTA is adjusted by the potential applied to the entrance slit and the energy resolution is expected to be smaller than 1% of the pass energy. The angular resolution is estimated to be 5-7 degrees.

A typical image for observing the Kr MNN Auger electrons following the Kr  $3d$  photoionization is presented in Fig. 2. In this measurement, the Auger electrons in the energy range of 48-58 eV are measured. At first glance, four coaxial circles which correspond to individual Auger lines are clearly separated. The intervals of the Auger lines are almost 1 eV. The Auger electron spectrum is deduced from the image, by summing the intensity along the radial direction. From Fig. 2, it is safe to say that the spectral resolution is better than 1 eV at the pass energy of 80 eV. In angular distributions, the concentric circles in Fig. 2 are far from isotropic. This anisotropy is resulted from the analyzer transmission efficiency and the detection efficiency of PSD. The three insensitve regions are apparent on the image. They are induced by three supporting struts in the lens system. To measure angular distribution of ejected electrons, the transmission and the detection efficiency of the analyzer should be calibrated by observing the Auger/photoelectron which shows isotropic angular distribution.

Our next plan is to develop an electron-ion coincidence spectrometer by combining DTA with an ion momentum spectrometer [2]. The coincidence spectrometer is under construction and will be applied to observe anisotropic electron emissions in a molecular frame.

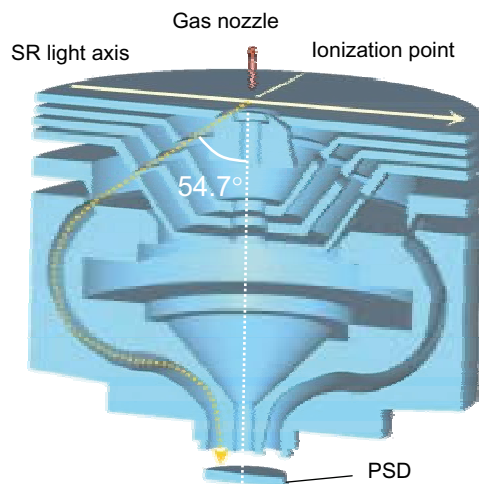


Fig. 1 Schematic drawing of DTA. DTA is equipped with the two-dimensional PSD, which provides energy and angular distributions of electrons.

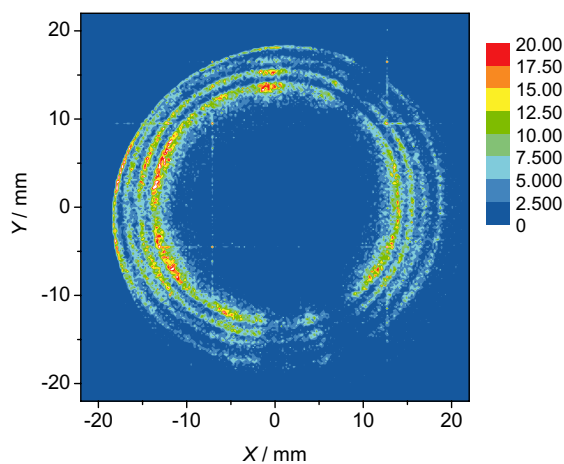


Fig. 2 Two-dimensional image of Kr MNN Auger electrons following Kr  $3d$  photoionization. DTA was operated with the electron pass energy of 80 eV. Four concentric circles on the image are attributed to the Auger lines and their energy intervals are almost 1 eV.

[1] C. Miron *et al.*, *Rev. Sci. Instrum.* **68** (1997) 3728.

[2] T. Kaneyasu *et al.*, in this report.

## Efficient Production of Metastable Hydrogen Fragments around the Cl 2p Ionization Thresholds of HCl

E. Shigemasa<sup>1</sup>, M. Simon<sup>2</sup>, R. Guillemin<sup>2</sup>, T. Kaneyasu<sup>1</sup>, Y. Hikosaka<sup>1</sup>

<sup>1</sup>*UVSOR Facility, Institute for Molecular Science, Okazaki 444-8585, Japan*

<sup>2</sup>*Laboratoire de Chimie Physique - Matière et Rayonnement (LCPMR), Université Pierre et Marie Curie, 11 rue Pierre et Marie Curie, 75231 PARIS Cedex 05, France*

Multielectron processes, in which more than two electrons are promoted by the absorption of a single photon, have long drawn special attention in the research field of atomic and molecular inner-shell physics. The multielectron processes are known to happen not only in the primary inner-shell hole creation processes, but also in their relaxation processes.

Recently some trial experiments have been made for observing minor products, such as highly excited neutral species and anions after the molecular inner-shell excitations, in order to find a direct probe for investigating the multielectron processes. A strong enhancement due to the N\* formation has been observed around the 1s threshold of N<sub>2</sub> molecules [1]. It has been found that the highly excited N<sub>2</sub><sup>+</sup>\* states leading to the N\* formation are populated by spectator Auger decay from the core-excited states, as well as by the recapture of slow photoelectrons into the Rydberg orbitals. It turns out that the metastable observation is a new and sensitive probe to study the decay dynamics of core-excited states and the photoelectron recapture due to the post-collision interaction. Neutral particle formation in the K-shell excitation regions of O<sub>2</sub>, CO, and NO has also been investigated and similar enhancements of the neutral particle yields around all the thresholds have been observed. Metastable fragment emission seems to be a common process on the decay of high-n Rydberg states in molecular inner-shell regions.

Here, preliminary results on the neutral fragment formation near the Cl 2p ionization thresholds of HCl molecules are presented. The experiment was carried out on BL4B, by using a simple MCP detector with retarding grids. Figure 1 shows the neutral and ion yield curves in the vicinity of the Cl 2p ionization thresholds. The peak structures in the lower photon energy region correspond to the Rydberg states. The clear differences between the two curves are detected around the thresholds; two broad features are observed only in the neutral yield curve. A direct evidence for producing metastable fragments can be gained by performing the coincidence detection between metastable and ionic fragments, which can also lower the fluorescence contribution in the neutral yield curve considerably. It has turned out that only the H\*/Cl<sup>n+</sup> coincidence signals are detectable. The H\*/Cl<sup>n+</sup> coincidence yield curve near the Cl 2p ionization region of HCl is exhibited in Fig. 2. In comparison to the red curve in Fig. 1 and the blue one

in Fig. 2, the sufficient reduction of the fluorescence contribution is evident. It is nicely demonstrated that the H\* fragments are efficiently produced mainly just around the Cl 2p ionization thresholds. The HCl<sup>+</sup>\* states produced by the spectator Auger decay from the core-excited states, as well as by the recapture of the slow photoelectrons into the Rydberg orbitals play an important role for the efficient H\* formation near the thresholds. Similar investigation for the Cl 1s ionization region has been attempted on BL1A, but no practical result has been obtained, due to the low photon intensity around 2.8 keV.

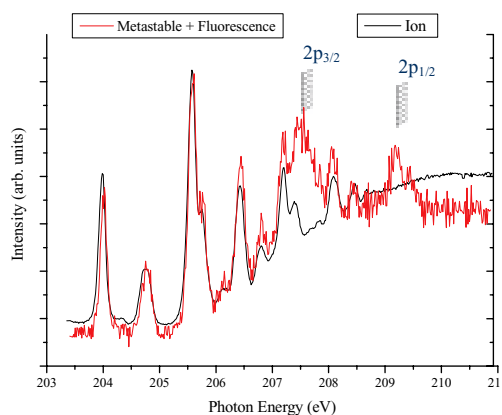


Fig. 1 Neutral and ion yield curves near the Cl 2p ionization region of HCl.

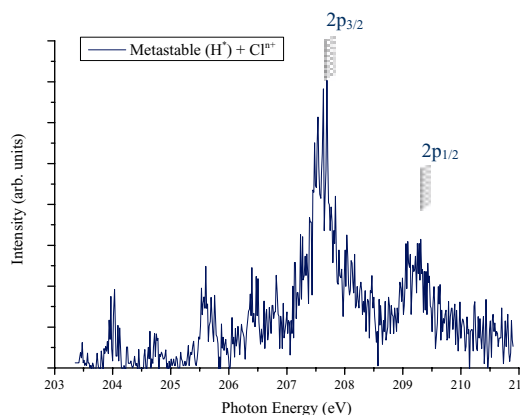


Fig. 2 H\*/Cl<sup>n+</sup> coincidence yield curve near the Cl 2p ionization region of HCl.

[1] Y. Hikosaka, P. Lablanquie, and E. Shigemasa, *J. Phys. B* **38**, (2005) 3597.